

BRITISH GEOLOGICAL SURVEY

REPORT No. IR/01/099

**METAMORPHISM OF THE LOWER PALAEOZOIC
ROCKS OF THE LEADHILLS DISTRICT,
SOUTHERN SCOTLAND, 1:50K Sheets 15E and 23E**

S J Kemp & R J Merriman

Date

10th May 2001

Classification

Open

Geographical index

Southern Scotland

Subject index

Low grade metamorphism, mica crystallinity, burial.

Bibliographic reference

Kemp, S.J. & Merriman, R.J 2001. Metamorphism of the Lower Palaeozoic rocks of the Leadhills district, southern Scotland, 1:50K Sheets 15E and 23E. *British Geological Survey Report IR/01/099*

CONTENTS

	Page
1 INTRODUCTION.....	1
2 TECHNIQUES AND LABORATORY METHODS	2
2.1 Techniques	2
2.2 Sample preparation.....	2
2.3 X-ray diffraction analysis.....	3
3 METAMORPHIC MAP.....	3
4 METAMORPHIC HISTORY.....	5
5 REFERENCES.....	8

FIGURES

Figure 1. Contoured metamorphic map of white mica crystallinity (Kubler) indices for Sheet 15E.....	10
--	-----------

APPENDIX

Summary of sample numbers, sample locations and KIs	11
--	-----------

BRITISH GEOLOGICAL SURVEY**REPORT No. IR/01/099****METAMORPHISM OF THE LOWER PALAEOZOIC ROCKS OF THE
LEADHILLS DISTRICT, SOUTHERN SCOTLAND, 1:50K Sheets 15E and 23E****S J Kemp and R J Merriman****1 INTRODUCTION**

Systematic studies of metapelitic grade linked with the geological re-survey of the Southern Uplands have been used to generate a series of contoured metamorphic maps which currently cover nearly two-thirds of the Lower Palaeozoic terrane. These studies have used X-ray diffraction (XRD) measurements of clay mineral reaction progress, particularly white mica (illite) crystallinity, to delineate zones of diagenesis and low-grade metamorphism in the imbricated Ordovician and Silurian strata. Although the regional pattern revealed by metapelitic zonal sequences shows considerable variations in metamorphic trends, patterns of increasing grade from older into younger strata suggest that accretionary burial was the main cause of regional metamorphism (Merriman & Roberts, *in press*). These patterns also reflect the different levels of exhumation of the terrane, by both normal movement on reactivated thrust faults and differential block movement on north-north-west-trending faults.

During the recent re-survey of the Leadhills district, metapelitic rocks representative of the main tectonostratigraphical units were collected and used to determine white mica (illite) crystallinity indices. This report gives details of the methods used and presents the results as a contoured metamorphic map which is used to interpret the metamorphic history of the district.

2 TECHNIQUES AND LABORATORY METHODS

2.1 Techniques

Burial of unconsolidated clays in basinal sequences causes progressive compaction and lithification resulting in typical shale and mudstone lithologies. The clay mineral reactions that accompany lithification transform authigenic minerals, such as smectite and kaolinite, to assemblages dominated by illite and chlorite. Tectonic deformation of these pelitic lithologies results in further progressive changes in clay mineral assemblages and the development of metapelites with a slaty cleavage microfabric. Progress of late diagenetic and very low grade metamorphic reactions in buried and tectonized pelitic sequences can be monitored by measuring changes in the illite–muscovite (white mica) reaction series as thicker crystallites develop in response to progressive recrystallisation (Merriman *et al.*, 1990, 1995; Warr & Rice, 1994). The Kubler index (KI in $\Delta^{\circ}2\theta$) measures small reductions in the half-height width of the mica ~ 10 Å XRD peak which occur when the crystallite population thickens. In pelitic rock sequences the Kubler index is used to define the limits of a series of metapelitic zones of very low– and low-grade metamorphism: late diagenetic zone KI>0.42; lower anchizone KI 0.30–0.42; upper anchizone KI 0.25–0.30; epizone KI<0.25 (Merriman & Peacor, 1999).

For this study, 180 metapelite samples were collected from the area south of the Southern Upland Fault (SUF) mainly within Sheets 15E and 23E with some overlap onto Sheet 16W to the east and Sheet 9E to the south. This represents a sampling density of approximately 1 metapelite per 2.5 km². All samples were prepared and analysed by XRD techniques in order to determine the Kubler Index (KI) of white mica (illite) crystallinity.

2.2 Sample preparation

Initial sample crushing was carried out by the BGS Sample Preparation Facility, Keyworth. After removing any surface contaminants with a wire brush, a representative 50 g portion of each sample was stage-ground, using a Cr-steel tema-mill in 5 second bursts, to pass a 1 mm sieve. Care was taken to subject the sample to short bursts of milling in order to reduce the chance of

over-grinding the delicate phyllosilicates.

A representative 4 g portion of each <1 mm crushed sample was then placed in a boiling tube and distilled water added to a predetermined level. Each sample was then shaken thoroughly, subjected to ultrasound for 5 minutes and allowed to stand for 3 hours. Where flocculation occurred, 0.5 ml of 0.1M sodium hexametaphosphate was added and the dispersion process repeated. After 3 hours, a nominal <2 μm fraction was removed and centrifuged at maximum speed for 20 minutes. The clear supernatant was then removed and the <2 μm fraction re-dispersed in ~1 ml distilled water with a glass rod and minimal ultrasound. The <2 μm fraction slurry was then pipetted onto the surface of a frosted glass slip and allowed to dry overnight at room temperature.

2.3 X-ray diffraction analysis

Each glass slip was analysed using a Philips PW1130 series diffractometer equipped with Ni-filtered Cu-K α radiation and operating at 40kV and 30mA. The KIs of the samples were calculated from the mean of five scans over the range 7.5-10.5 $^{\circ}2\theta$ at a speed of 0.5 $^{\circ}2\theta/\text{minute}$ using the machine conditions recommended by Kisch (1991). The width of the ~10 Å peak at half-height was measured using either Hiltonbrooks software modified by N J Fortey (BGS) or the graphics package within Philip's X'Pert software suite. In both cases, values were adjusted to concur with previous measurements carried out at Birkbeck College, University of London. A summary of sample numbers, locations and KIs are shown in the Appendix of this report.

3 METAMORPHIC MAP

The metamorphic map shown in Figure 1 is the result of a computer-contoured plot of KI data, which was subsequently manually modified to reflect the influence of localized post-regional metamorphic events. A computer contoured geographical distribution of KI datapoints was initially produced using Deltagraph 4.0 for Windows software. The pattern was then superimposed on an outline 1:50k geological map of the Lower Palaeozoic strata and contours redrawn where thermal overprinting and post-metamorphic faulting appeared to modify the

overall pattern. In the final version of the map shown in Figure 1, contours of equal crystallinity (isocrysts) are used to delineate four metapelitic zones: late diagenetic zone (KI >0.42); lower anchizone (KI 0.30–0.42); upper anchizone (KI 0.24–0.30) and epizone (KI <0.24). In order to link with published maps for adjacent sheets the intervals used differ slightly from those described in section 2. The errors and precision involved in contouring the crystallinity data (Robinson *et al.*, 1990) were previously determined by multi-sampling at several sites in the Southern Uplands (Merriman & Roberts, 1992) and elsewhere (Roberts *et al.*, 1990). The results from multi-sampled sites indicate that 95% of the samples have indices within the range of values delineated by zonal isocrysts.

The contoured metamorphic map shows a regional pattern that is characterised by the sub-parallelism of isocrysts with the regional strike, and by abrupt changes in grade across the strike-parallel, tract-bounding faults. This is a common pattern across the Southern Uplands terrane, and indicates a close relationship between the imbrication of the succession and regional metamorphism (Merriman & Roberts, *in press*). The regional pattern is overprinted by a relatively narrow contact aureole which is generally concentric with the Spango Water intrusion. A system of late north-north-west-trending faults through the centre of the district, associated with the development of Upper Palaeozoic basins at Thornhill and Snar Valley, has also modified the regional pattern. Movement on the fault system, referred to as the Durisdeer Fault Zone, has resulted in different levels of exhumation of the Lower Palaeozoic rocks (Merriman & Roberts, *in press*), and is reflected in overall differences in grade in the eastern and western parts of the district.

The highest grade strata crop out in the east of the district, on the upthrown side of the Durisdeer Fault Zone. In this area, between the Southern Upland Fault and the Orlock Bridge Fault, grade generally increases from older into younger rocks. On crossing the Orlock Bridge Fault grade again increases into the epizonal rocks that form an extension of the Moniaive Shear Zone (MSZ), cropping out to the east of the Thornhill Basin. South-east of the MSZ, grade decreases into sequentially younger rocks. The local pattern of metamorphism adjacent to the epizonal rocks of the MSZ differs from that found around Moniaive, on Sheet 9W (British Geological Survey, 1998). To the east of the Thornhill Basin, relatively high grade (high-anchizone) rocks

are found to the north-west of the MSZ, whereas around Moniaive up to 4 km of downthrow on the Orlock Bridge Fault has juxtaposed late diagenetic grade strata against the epizonal rocks of the MSZ (McMillan, *in press*; Merriman & Roberts, *in press*). Such differences suggest that post-shearing downthrow on the Orlock Bridge Fault was locally less than 1 km, and that to the north-east of the Thornhill Basin the Orlock Bridge Fault is inclined to the north-west, in contrast to its steep or vertical attitude in the south-west of the terrane (Barnes et al., 1995; Merriman & Roberts, *in press*).

To the west of the Thornhill Basin, grade is generally in the late diagenetic zone or low-anchizone and shows no systematic changes in relation to the tectonostratigraphy. A restricted area of high-anchizone and epizonal strata is found to the south of Wanlockhead, immediately west of the Durisdeer Fault Zone. This appears to be an extension of the high-anchizone rocks on the eastern upthrown side of the fault zone, and is probably the result of rotation of the downthrown block.

4 METAMORPHIC HISTORY

The pattern of regional metamorphism developed in the Lower Palaeozoic rocks of the Leadhills district can be interpreted in terms of four tectonometamorphic events that have contributed to the evolution of the Southern Uplands terrane (Merriman & Roberts, *in press*):

1. Regional very low-grade metamorphism resulting from accretionary burial
2. Localized shear zone metamorphism associated with the MSZ
3. Contact metamorphism associated with late granitic intrusions
4. Uplift and block faulting prior to Permo-Carboniferous basin development

Evidence for accretionary burial is generally confined to the area east of the Durisdeer Fault Zone where the oldest strata forming the Marchburn Formation (Tappins Group) are generally at lower grades than the younger strata of the Barrhill Group. Similar relationships were observed on the Rhins of Galloway and in the Carrick district (Merriman & Roberts, 1992; Stone, 1995; Hirons *et al*, 1997). Such patterns indicate that younger strata were emplaced beneath older strata

and in turn this suggests that the metamorphic pattern was generated by accretion-related tectonism (Merriman & Frey, 1999; Merriman & Roberts, *in press*). Patterns of this type would be expected if the north-westward-younging Barrhill Group were sequentially underthrust and buried beneath the older Tappins Group. The latter may have formed the upper level of a thrust stack which is now preserved by downfaulting associated with late tensional reactivation of the Southern Upland Fault.

The extension of the MSZ cropping out on the east side of the Thornhill Basin is atypical in having relatively high grade rocks on the north-western side of the zone. Such a pattern would be expected elsewhere along the MSZ, but for the large downthrow on the Orlock Bridge which truncates the MSZ along much of its outcrop. However, in the Leadhills district, a smaller downthrow (<1 km) on the Orlock Bridge Fault has preserved areas of high-anchizonal and epizonal rocks that originally formed the hanging wall of the fault. Much of the lead-zinc mining area of Leadhills and Wanlockhead occurs within these rocks, suggesting that initial enrichment of these metals may have been associated with fluids generated within and adjacent to the zone of shearing.

Late granitic intrusions into the Lower Palaeozoic rocks occur in the northwest of the district, at Spango Water, and as a thin, strike-parallel dyke-like body within the MSZ trending northeast across Ballencleugh Law. The thermal aureole around the Spango intrusion overprints the regional pattern in the Marchburn and Kirkcolm formations, and was probably generated during emplacement at depths of 6-8km in the upper level of the Southern Uplands thrust stack (Merriman & Roberts, *in press*). Localised geochemical enrichment in trace elements Ba, Cu, Ni, Pb and Zn appears to be associated with the aureole (British Geological Survey, 1993), suggesting that hydrothermal activity associated with the cooling intrusion may have scavenged these and other elements from the country rocks. Due to poor exposure and the relatively high grade within the MSZ, no aureole could be distinguished around the Ballencleugh Law dyke. Ni and Zn enrichment appears to be associated with this intrusion (British Geological Survey, 1993).

Post-metamorphic uplift of the terrane led to localised reactivation of thrusts as normal faults and also to block movement along north-north-west-trending faults. Movement on both sets of faults is responsible for the present pattern of metamorphism. The contrast in grade across the district is due to differential block movement along the Durisdeer Fault Zone which has exhumed the upper and lower levels of accreted strata comprising the Southern Uplands thrust stack (Merriman & Roberts, *in press*). Downthrow to the west of the fault zone has preserved the lower grade strata that originally formed the upper level of the Southern Uplands thrust stack. To east of the fault zone, the exhumed MSZ and associated higher grade rocks represent the deeper underplated level of the thrust stack. Much of the Leadhills-Wanlockhead mining district is developed along and to the east of the fault zone, within the relatively high grade rocks that initially formed the hanging wall of the Orlock Bridge Fault.

5 REFERENCES

BARNES, R.P., PHILLIPS, E.R. & BOLAND, M.P. 1995. The Orlock Bridge Fault in the Southern Uplands of southwestern Scotland: a terrane boundary? *Geological Magazine*, **132**, 523-529.

BRITISH GEOLOGICAL SURVEY. 1993. *Regional geochemistry of southern Scotland and part of northern England*. (Keyworth, Nottingham: British Geological Survey).

HIRON, S.R., ROBERTS, B. & MERRIMAN, R.J. 1997. Metamorphism of the Lower Palaeozoic rocks of the Carrick–Loch Doon region, southern Scotland. *British Geological Survey Technical Report*, **WG/97/25**.

KISCH, H.J. 1991. Illite crystallinity: recommendations on sample preparation, X-ray diffraction settings and interlaboratory standards. *Journal of Metamorphic Geology*, **9**, 665-670.

McMILLAN, A. (*in press*). The New Galloway–Thornhill district: a concise account of the geology. *Memoir of the British Geological Survey*, Sheets 9W & 9E (Scotland).

MERRIMAN, R.J. & ROBERTS, B. 1992. The low grade metamorphism of Lower Palaeozoic strata on the Rhins of Galloway, SW Scotland. *British Geological Survey Technical Report* **WG/92/40**.

MERRIMAN, R.J. & FREY, M. 1999. Patterns of very low–grade metamorphism in metapelitic rocks. In: FREY, M. & ROBINSON, D. (eds) *Low–grade Metamorphism*. Blackwell Science, pp 61-107.

MERRIMAN, R.J. & PEACOR, D.R. 1999. Very low–grade metapelites: mineralogy, microfabrics and measuring reaction progress. In: FREY, M. & ROBINSON, D. (eds) *Low–grade Metamorphism*. Blackwell Science, pp 10-60.

MERRIMAN, R.J. & B ROBERTS, B. (in press). Low-grade metamorphism in the Scottish Southern Uplands terrane: deciphering the patterns of accretionary burial, shearing and cryptic aureoles. *Transactions of the Royal Society of Edinburgh: Earth Sciences*,

MERRIMAN, R.J., ROBERTS, B. & PEACOR, D.R. 1990. A transmission electron microscope study of white mica crystallite size distribution in a mudstone to slate transitional sequence, North Wales, U K. *Contributions to Mineralogy and Petrology*, **10**, 27-40.

MERRIMAN, R.J., ROBERTS, B., PEACOR, D.R. & HIRONS, S.R. 1995. Strain-related differences in the crystal growth of white mica and chlorite: a TEM and XRD study of the development of metapelitic microfabrics in the Southern Uplands thrust terrane, Scotland. *Journal of Metamorphic Geology*, **13**, 559–576.

ROBERTS, B., MORRISON, C. & HIRONS, S. 1990. Low grade metamorphism of the Manx Group, Isle of Man: a comparative study of white mica ‘crystallinity’ techniques. *Journal of the Geological Society of London*, **147**, 271-277.

ROBINSON, D., WARR, L. & BEVINS, R.E. 1990. The illite ‘crystallinity’ technique: a critical appraisal of its precision. *Journal of Metamorphic Geology*, **8**, 333-344.

STONE, P. 1995. The Geology of the Rhins of Galloway District. *Memoir of the British Geological Survey*, Sheets 1 and 3 (Scotland).

WARR, L. & RICE, A.H.N. 1994. Interlaboratory standardization and calibration of clay mineral crystallinity and crystallite size data. *Journal of Metamorphic Geology*, **12**, 141–152.

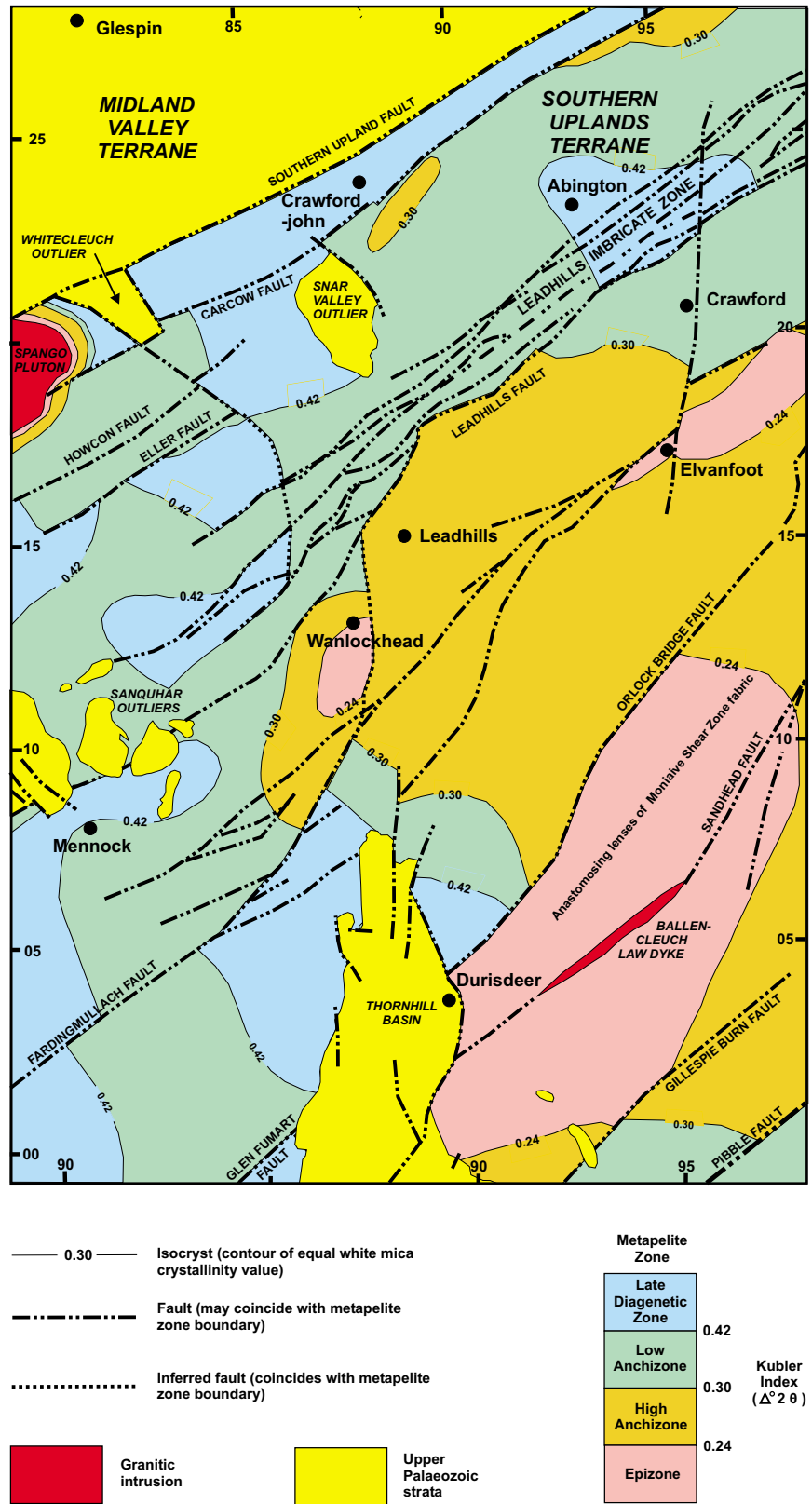


Figure 1. Contoured metamorphic map of white mica crystallinity (Kubler) indices for Sheet 15E.

APPENDIX: Summary of sample numbers, sample locations and KIs

Sample No.	Square	Easting	Northing	IC	Sample No.	Square	Easting	Northing	IC
AX2712	NS	294970	613490	0.29	EPT170	NS	283100	603390	0.41
AX2713	NS	294240	621460	0.30	EPT171	NS	280460	608240	0.43
AX2721	NS	291050	604250	0.32	EPT172	NS	280780	607740	0.38
AX2724	NS	292830	605530	0.23	EPT174	NS	283280	605930	0.41
AX2732	NS	296000	601700	0.31	EPT175	NS	283770	605300	0.46
AX2710	NS	292650	620540	0.31	EPT177	NS	284290	605290	0.54
AX2711	NS	294240	621460	0.76	EPT179	NS	287010	608010	0.50
AX2798	NS	292190	618970	0.32	EPT180	NS	287570	608650	0.33
AX2799	NS	292150	618980	0.30	EPT182	NS	286100	606200	0.55
AX2800	NS	293730	621750	0.51	EPT191	NS	283110	609610	0.80
AX2804	NS	290800	617800	0.32	EPT193	NS	289340	606430	0.42
AX2805	NS	290340	618270	0.26	EPT194	NS	285510	608680	0.25
AX2807	NS	291510	617000	0.29	EPT197	NS	285680	600470	0.37
AX2811	NS	288710	616530	0.26	EPT198	NS	281180	602110	0.41
AX2812	NS	288430	616520	0.24	EPT205	NS	283060	606880	0.27
AX2818	NS	287310	617020	0.34	EPT206	NS	290000	602980	0.24
AX2821	NS	286270	616500	0.39	ETS454	NS	284410	620410	NA
AX2853	NS	285830	618900	0.44	ETS455	NS	283620	621990	0.48
AX2854	NS	286490	617870	0.38	ETS456	NS	283130	620590	0.38
AX2858	NS	288290	617130	0.32	ETS457	NS	280750	620870	1.09
AX2859	NS	289520	617030	0.24	ETS550	NS	289170	625040	0.50
AX2862	NS	289320	617810	0.26	ETS551	NS	286910	623600	0.41
AX2866	NS	287820	618370	0.36	ETS552	NS	287240	622480	0.35
AX2867	NS	287110	619150	0.45	ETS553	NS	286420	620470	0.57
AX2869	NS	291460	619640	0.31	ETS554	NS	289180	623850	0.29
AX2874	NS	291920	623810	0.43	ETS555	NS	282790	619780	0.24
BRS874	NX	282100	599800	0.35	ETS556	NS	284430	619570	0.50
BRS1204	NS	280600	615380	0.45	ETS557	NS	281990	618290	0.31
BRS1208	NS	280200	617300	0.34	ETS558	NS	283100	617240	0.33
BRS1209	NS	285430	623400	1.15	ETS560	NS	283390	615710	0.36
BRS1216	NS	288000	613290	0.27	ETS561	NS	284040	616070	0.56
EPT083	NS	284780	608380	0.33	ETS564	NS	280960	616250	0.39
EPT085	NS	284100	608660	0.32	HFB 118	NS	296020	627660	0.30
EPT087	NS	284160	607600	0.46	HFB 131	NS	297250	625930	0.34
EPT088	NS	283170	608220	0.37	HFB 133	NS	296760	627060	0.32
EPT089	NS	286640	609990	0.31	HFB 134	NS	296650	626300	0.40
EPT090	NS	285680	609680	0.26	HFB 135	NS	296290	625190	0.30
EPT095	NS	285690	607320	0.34	HFB 136	NS	294930	626230	0.35
EPT097	NS	289990	608430	0.30	HFB 137	NS	297230	625010	0.27
EPT099	NS	289310	609530	0.20	HFB 145	NS	298350	625600	0.31
EPT102	NS	281980	608710	0.53	HFB 146	NS	298780	626410	0.36
EPT103	NS	283940	609910	0.39	HFB 147	NS	297880	625720	0.32
EPT107	NS	288600	607750	0.34	HFB 148	NS	295190	627460	0.27
EPT109	NS	288400	609540	0.27	HFB177	NS	291920	626790	0.38
EPT159	NS	280240	603330	0.45	HFB178	NS	292850	626370	0.30
EPT162	NS	280800	602950	0.37	HFB179	NS	291820	625920	0.33
EPT165	NS	283580	604110	0.35	HFB181	NS	292390	625060	0.38
EPT167	NS	282530	604500	0.37	HFB183	NS	293640	627210	0.47
EPT168	NS	282640	602670	0.41	HFB185	NS	293870	625210	0.38

APPENDIX: Summary of sample numbers, sample locations and KIs (continued)

Sample No.	Square	Easting	Northing	IC	Sample No.	Square	Easting	Northing	IC
HFB187	NS	294160	626670	0.39	RJM638	NS	292870	602620	0.26
HFB189	NS	294520	627300	0.25	RJM639	NS	290600	602440	0.39
HFB222	NS	297000	622930	0.33	RJM640	NS	289970	600220	0.22
HFB225	NS	297210	623850	0.33	RJM641	NS	295700	617780	0.23
HFB230	NS	296470	624200	0.42	RJM642	NS	296130	616970	0.22
HFB232	NS	298540	624320	0.41	RJM643	NS	298030	616100	0.28
HFB240	NS	295580	622670	0.43	RJM644	NS	299250	615350	0.28
HFB241	NS	295320	622020	0.25	RJM659	NS	281780	609930	0.38
HFB243	NS	297820	619320	0.22	RJM660	NS	280040	611440	0.38
HFB244	NS	296270	620800	0.34	RJM661	NS	279900	613210	0.36
HFB259	NS	295010	617300	0.23	RJM662	NS	280780	614570	0.39
HFB266	NS	295480	624530	0.38	RJM663	NS	281890	613480	0.44
RJM600	NX	297170	599310	0.77	RJM664	NS	281850	617710	0.43
RJM601	NS	297090	600530	0.32	RJM665	NS	282420	616580	0.52
RJM602	NS	296310	600190	0.29	RJM666	NS	282420	616580	0.51
RJM603	NS	290270	604580	0.18	RJM667	NS	283000	615370	0.29
RJM604	NS	290270	604580	0.22	RJM668	NS	283200	614390	0.34
RJM605	NS	291480	605800	0.23	RJM669	NS	287890	622070	0.29
RJM606	NS	291210	605980	0.23	RJM670	NS	288900	621170	0.34
RJM607	NS	290670	605920	0.44	RJM671	NS	287360	611220	0.24
RJM608	NS	290670	605920	0.36	RJM672	NS	287250	612300	0.20
RJM609	NS	290670	605920	0.49	RJM673	NS	284700	614150	0.42
RJM610	NS	289950	604960	0.53	RJM674	NS	285470	614600	0.45
RJM611	NS	290000	603000	0.27	RJM675	NS	285190	615290	0.34
RJM612	NS	290900	608270	0.29	RJM676	NS	289270	615020	0.25
RJM613	NS	292690	607830	0.19	RJM677	NS	292480	615780	0.24
RJM614	NS	292470	608520	0.25	RJM678	NS	293480	612500	NA
RJM615	NS	296390	611900	0.33	RJM679	NS	293700	612330	0.27
RJM616	NS	296300	610720	0.20	RJM680	NS	297910	611350	0.26
RJM617	NS	298000	609200	0.24	RJM681	NS	295580	606680	0.21
RJM619	NS	296720	609020	0.22	RJM691	NS	296300	614450	0.44
RJM620	NS	296270	607720	0.22	RJM692	NS	296850	613400	0.25
RJM621	NS	295640	608880	0.41	RJM693	NS	297000	614500	0.25
RJM622	NS	294900	608700	0.19	RJM694	NS	296700	614900	0.26
RJM623	NS	295650	605030	0.21					
RJM624	NS	294930	604910	0.25					
RJM625	NS	294490	604980	0.20					
RJM626	NS	294490	604980	0.21					
RJM627	NS	295520	602300	0.25					
RJM628	NS	296180	604310	0.25					
RJM629	NS	295490	615300	0.28					
RJM630	NS	293210	617590	0.28					
RJM631	NS	292200	617190	0.29					
RJM632	NS	290020	615480	0.27					
RJM633	NS	288300	611690	0.27					
RJM634	NS	290040	612070	0.27					
RJM635	NS	291240	602240	0.23					
RJM636	NS	292600	600790	0.22					
RJM637	NS	292830	602120	0.24					